Proceeding of the IEEE
International Conference on Robotics and Biomimetics
Dali, China, December 2019

Master-slave control strategy for minimally invasive surgery with a fast inverse kinematics solution

Zhuangzhuang Zhang, Qixin Cao, Pengfei Wang, Guohan He
School of Mechanical Engineering
Shanghai Jiao Tong University
Shanghai, China
ZhangZZ616296@163.com

Tiewen Pan
Department of Thoracic Surgery
Eastern Hepatobiliary Surgery Hospital
Shanghai, China
pantw118@163.com

***Abstract*— In this work we present a teleoperation for a surgical robot with a fast inverse kinematics solution. The work contains a full robot kinematics model and the teleoperation process. The errors that occurred in the establishment of the inverse kinematics model are analyzed in detail and corresponding compensation measures are given. A robot operating system (ROS) interface has been created for easy use and development of common software components. Moreover, several scenes have been implemented to illustrate the performance and potentiality of the developed algorithm.**

***Index Terms*— surgical robot, teleoperation, a fast inverse kinematics solution.**

I. Introduction

Today, minimally invasive surgery (MIS) becomes more and more popular among both surgeons and patients. The related technologies are attracting great attention from many researchers all over the world. Many prototypes and practical products have been successfully developed and achieved great success in clinical practice. These include the well-known da Vinci Surgical System [1][2], Chinese minimally invasive surgical robot system "Micro Hand S" [3][4]. ZEUS robotic system [5]. Among these surgical robots, the da Vinci surgical robotic system is the most successful commercial system. To date, there are more than 5000 da Vinci surgical robotic systems have been installed and in use in hospitals throughout the world. At present, the total number of patients treated with Da Vinci surgical system has exceeded 5 million worldwide [6]. Vinci surgical robotic system can provide a clear and enlarged 3D view and the manipulator is smaller than the human hand which can filter hand vibration during direct operation. However, at present, the purchase cost and annual service cost of the surgical robot are high, and the operation cost is also expensive, which limits the application of the da Vinci Surgical System in developing countries such as China. To reduce costs and deliver more contributions to the Chinese healthcare, we have been developing a surgical robot system, as in Fig. 1, it was named as "HuaTuo II". Similar to the most surgical system, "HuaTuo II" is a master-slave robot. It contains four manipulators as slave, two omega7 devices as master. The two master manipulators

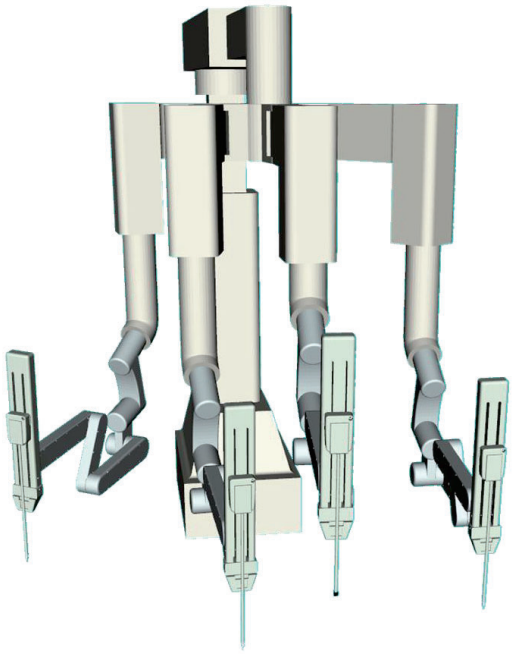

Fig. 1. Overview of the surgical robot platform.

are the motion input devices, for one master manipulator, there are seven degrees of freedom which contains three axis position, three axis orientation and one grip degree of freedom. It can transmit position and orientation in cartesian space to the slave manipulators via electrical signals. The signals are used to control slave manipulators and instruments to finish surgical operation inside the patient's body. Because the master manipulator omega7 devices are existing products, so we mainly focus on features of the slave manipulators. The slave cart consists of four slave manipulators. They are two surgical arms, one endoscope arm and one spare arm. We can also divide the whole robot kinematics into three parts, namely Setup joints (SUJ), Patient Side Manipulators (PSMs), Endoscopic Camera Manipulator (ECM) [2]. On the other hand, this division is also helpful for us to carry out

978-1-7281-6321-5/19//$31.00 ©2019 IEEE

kinematics modeling. The SUJ for whole slave cart has four active joints, The SUJ for each slave manipulator has three active joints, each PSM has eight degrees of freedom which include four degrees of freedom from instruments. Seven degrees of freedom of PSM are used to connect with the master signals to perform the teleoperation operation. The ECM has four degrees of freedom which is used to adjust position of the endoscope. The structure of ECM is same as PSM except instruments. In other words, the kinematic model of ECM is a part of the PSM.

The rest of the paper is organized as follows: In Sect. II the forward and inverse kinematics of the robotic arms are described; in Sect. III the error of inverse kinematic is discussed and compensation measures are presented; Section IV describes teleoperation operation process and the control architecture focusing on the ROS based infrastructure; in Sect. V we discuss several different scenes developed in the simulated environment as proof of concept to show the potentialities of the proposed algorithm. Sect. VI concludes the paper.

II. Full Kinematics Model

There are usually two ways of representing a robot kinematic model, they are DH method and homogeneous coordinate method [7], respectively. Due to the drawbacks of DH parameter method, such as, we could not use DH parameter method when a joint motion around y-axis [8]. Therefore, homogeneous coordinate method is adopted to establish a unified kinematics model.

A. Forward Kinematics

The definition of homogeneous transformation is shown in the appendix. The relationship between two adjacent joints can be described as a six-dimensional vector:

$$V = [x, y, z, \alpha, \beta, \gamma] \tag{1}$$

where α, β, γ are the rotation of the $i+1$ coordinate system with respect to the x, y, z axis of the i coordinate system, x, y, z are the translation of the $i+1$ coordinate system with respect to the x, y, z axis of the i coordinate system, the order of transformation from i to $i+1$ is α, β, γ, x, y, z, so we can get homogeneous transformation between joints coordinate:

$$\begin{aligned} Xyz[V] &= TransX(x) \cdot TransY(y) \cdot TransZ(z) \\ Rpy(V) &= RotZ(\gamma)) \cdot RotY(\beta)) \cdot RotX(\alpha)) \\ XyzRpy &= Xyz[V] \cdot Rpy(V) \end{aligned} \tag{2}$$

Then the transformation relationship from i to $i+1$ can be written as:

$$T_{i+1}^{i} = XyzRpy(V_i) \tag{3}$$

When link rotate θ around coordinate system $i+1$, the transformation relationship from i to $i+1$ can be written as:

$$T_{i+1}^{i} = XyzRpy(V_i) \cdot RotZ(\theta_{i+1}) \tag{4}$$

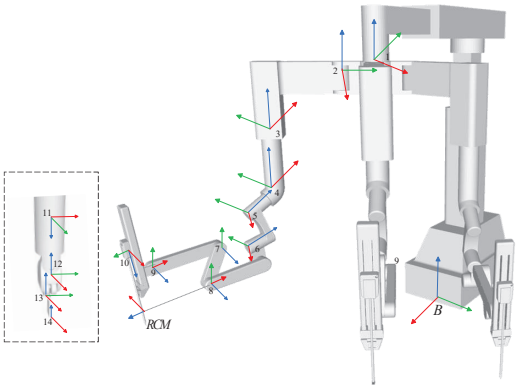

Fig. 2. Forward kinematic description.

Fig. 2 shows homogeneous coordinate system for each joint. M represents the initial homogeneous transformation matrix of the whole manipulator. Because we want the manipulator in a particular position when boot. Joint 1 to 5 will keep a fixed position which can be read from absolute encoder. Joint 6 to 13, total six degrees of freedom, will be controlled by the signals given by master device. We can write a complete forward kinematics expression which is simpler and easier to understand than DH expression.

The matrixs M shown in Table I. After establish transformation relationship between adjacent coordinate systems and initial homogeneous transformation matrix of the whole manipulator, the explicit expression for homogeneous transformation between joints can be written as:

$$T_{14}^{0} = T_{1}^{0} \cdot T_{2}^{1} \cdot T_{3}^{2} \cdots T_{13}^{14} \tag{5}$$

TABLE I
INITIAL HOMOGENEOUS TRANSFORMATION MATRIX

	x	y	z	α	β	γ
$M(0)$	0.657	0.044	1.815	0	0	1.571
$M(1)$	0	0.2	-0.03	0	0	1.74
$M(2)$	0	-0.420	-0.418	0	0	0.84
$M(3)$	-0.055	0	-0.365	0	0	0
$M(4)$	-0.132	0	-0.077	0	1.047	0
$M(5)$	0.1619	0	-0.113	0	0.2618	0
$M(6)$	0.060	-0.0025	-0.278	1.57	0.698	0
$M(7)$	-0.2	0	-0.0415	0	0	2.09
$M(8)$	-0.35	0	0.03	0	0	0
$M(9)$	-0.1	0.1	0.0085	0	-1.57	1.57
$M(10)$	0	0	0.3759	0	0	0
$M(11)$	0	0	0	3.14	0	1.57
$M(12)$	0	0.0003	-0.0089	0	0	2.09
$M(13)$	0	0	-0.0106	0	0	0

B. Inverse Kinematics

In order to keep real-time performance of Teleoperation [9][10][11], A fast analytical inverse solution method is

proposed. Our solutions are as follows: the effect of rotation of the three wrist joints at the end of the instrument on the spatial position of the surgical tools at the end of the instrument is neglected, and only the effect of the first three joints of the arm is considered. First step, we calculate the current joint control value of three joints on the upper arm based on the desired position at the end of the instrument, second step, solve the current angle value of the three wrist joints according to the desired posture at the end of the surgical tool and the three joint values given by first step. Thereby the analytical inverse solution of PSM can be obtained. We need to set an auxiliary coordinate system RCM (Remote Center of Motion) when solving the first three joint angles, as shown in Fig. 3, the figure represents the initial configuration of the robot. X-axis parallel to joint 2, Z-axis parallel to joint 1, the Y-axis is derived from the right-hand rule. Firstly, Cartesian position of instrument end effector is expressed in RCM coordinate system by forward kinematics:

$$\begin{aligned} T_{13}^{0} &= T_{1}^{0} \cdot T_{2}^{1} \cdots T_{10}^{9} \cdot T_{rcm}^{10} \cdot T_{13}^{rcm} \\ T_{13}^{rcm} &= (T_{rcm}^{0})^{-1} \cdot T_{13}^{0} \end{aligned} \tag{6}$$

We can easily get the values of first three joints through the geometric relations between coordinate systems:

$$\begin{aligned} d_8 &= \sqrt{x_{rcm}^2 + y_{rcm}^2 + z_{rcm}^2} \\ \theta_6 &= \arctan(x_{rcm}, y_{rcm}) \\ \theta_7 &= \arcsin(\frac{z_{rcm}}{d_8}) \end{aligned} \tag{7}$$

After solving the inverse kinematics of the first three joints, the angles of the remaining three wrist joints are calculated according to the desired posture of the end-effector. Based on previous calculations of forward kinematics, relationship can be written as:

$$\begin{aligned} &[\vec{n}_{13}, \vec{o}_{13}, \vec{a}_{13}, \vec{p}_{13}] = T_{13}^{0}\,(\theta_6, \theta_7, d_8, \theta_9, \theta_{10}, \theta_{11}) = \\ &T_1^0 \cdot T_2^1 \cdot T_3^2 \cdot T_4^3 \cdot T_5^4 \cdot T_6^5 \cdot Rot(\theta_6).T_7^6 \cdot Rot(\theta_7) \cdot \\ &T_8^7 \cdot Rot(-\theta_7).T_9^8 \cdot Rot(\theta_7) \cdot T_{10}^9 \cdot Rot(d_8).T_{11}^{10} \cdot \\ &Rot(\theta_9) \cdot T_{12}^{11} \cdot Rot(\theta_{10}).T_{13}^{12} \cdot Rot(\theta_{11}) \end{aligned} \tag{8}$$

where θ_6, θ_7, d_8 are given in first step, so they are treated as constants. Equation (8) can be rewritten as:

$$I = C \cdot T_{11}^{10} \cdot Rot(\theta_9) \cdot T_{12}^{11} \cdot Rot(\theta_{10}).T_{13}^{12} \cdot Rot(\theta_{11}) \tag{9}$$

where C is equal to:

$$\begin{aligned} C =& ([\vec{n}_{13}, \vec{o}_{13}, \vec{a}_{13}, \vec{p}_{13}])^{-1} \cdot T_1^0 \cdot T_2^1 \cdot T_3^2 \cdot T_4^3 \cdot T_5^4 \cdot \\ & T_6^5 \cdot Rot(\theta_6).T_7^6 \cdot Rot(\theta_7) \cdot T_8^7 \cdot Rot(-\theta_7).T_9^8 \cdot \\ & Rot(\theta_7) \cdot T_{10}^9 \cdot Rot(d_8) \end{aligned} \tag{10}$$

We can get three wrist values through further simplification formula, the detailed derivation process is not shown further.

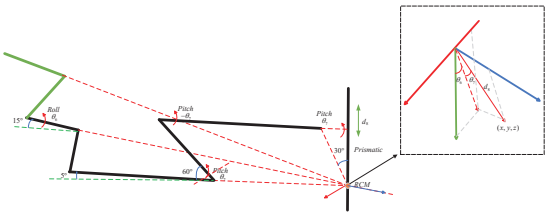

Fig. 3. RCM constraint relationship.

Three wrist values can be written as:

$$\begin{aligned} \theta_9 &= \arctan(\frac{c_{11}c_{33} - c_{13}c_{31}}{c_{13}c_{32} - c_{12}c_{33}}) \\ \theta_{10} &= \arctan(\frac{-c_{23}}{c_{21}\sin(\theta_9) + c_{22}\sin(\theta_9)}) \\ \theta_{11} &= \arcsin(-(c_{32}\cos(\theta_9)) - c_{31}\sin(\theta_9)) \end{aligned} \tag{11}$$

It should be noted that there are several groups of equivalent expressions for θ_9 , θ_{10}, θ_{11}, here we only choose one.

III. Error Analysis and Compensation

In the process of solving inverse kinematics, errors are introduced due to some assumptions made in the first step. The error is relatively small because the end of instrument is only 1cm, but for high accuracy in surgical operation. This section will evaluate the effect of the error caused by the two-step approximate solution on the accuracy of the end positioning.

A. Error Analysis

When using inverse kinematics expressions given by two-step approximate solution to control the slave hand, there is an error between the actual position at the end of the surgical instrument and the expected position because the influence of the rotation of the last three wrist joints on the spatial position at the end of the surgical instrument is ignored. Select a $6 \times 6 \times 6cm^3$ cube near the center of the workspace. The interval between adjacent points in each direction is 5mm. Taking these points as the expected position at the end of instrument, which is indicated by red dots in Fig. 4 (a), the first three angle values can be calculated based on the inverse kinematics, then the actual position of the end of instrument can be calculated out based on forward kinematics, which shows in Fig. 4 (a) as green dots, the maximum error reaches $7.4mm$. The relative error shows in Fig. 4 (b), maximum value reaches $3.2mm$.

B. Error Compensation

In order to improve the motion control accuracy of two-step approximate inverse kinematics algorithm as much as possible, we need to compensate the error in each control cycle to prevent the relative motion error from increasing with the increase of the motion distance. Thus, the motion

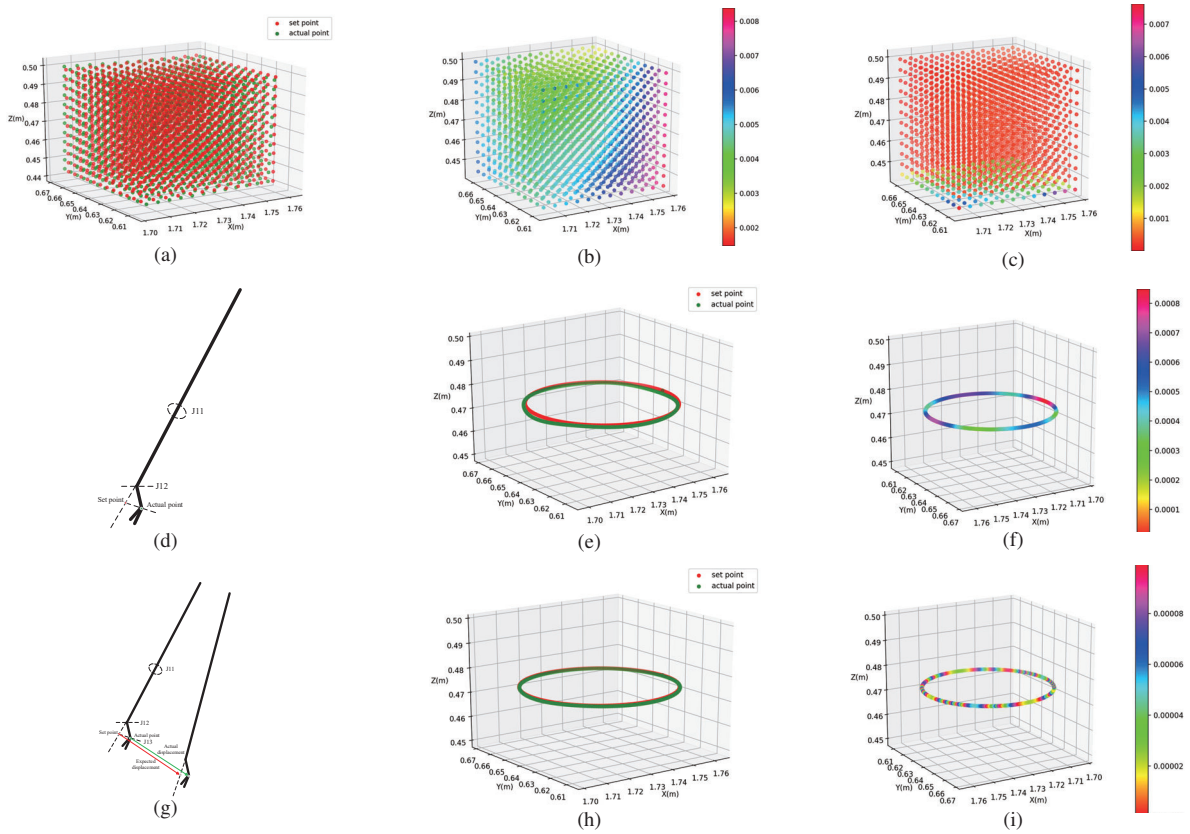

Fig. 4. Error and its compensation. (a): Display of desired and actual locations in the workspace. (b): The absolute error between desired and actual locations. (c): The relative error in every step. (d): Schematic diagram of expected position and actual position. (e): The absolute error before compensation. (f): The relative error before compensation. (g): Schematic diagram of error compensation. (h): The absolute error after compensation. (i): The relative error after compensation.

error introduced by the approximate algorithm is limited to the acceptable range for the surgical robot.

The compensation principle is shown in Fig. 4 (g). firstly, the value of command $\Delta\vec{d}_0^{target}$ and actual movement $\Delta\vec{d}_0^{actual}$ at the end of the surgical tool during the previous control period are known, where actual movement can be obtained by forward kinematics. The movement error for the previous control period can be obtained $\vec{e}_0 = \Delta\vec{d}_0^{target} - \Delta\vec{d}_0^{actual}$, by directly compensating the error to the current motion control, the corrected motion control command at the current moment can be obtained $\Delta\vec{d}_1^{actual} = \Delta\vec{d}_0^{actual} + \vec{e}_0$. In this way, the control quantity after compensation can correct the motion error at the previous moment. Similarly, the control quantity at the next moment can compensate the error generated at the current moment and proceed in sequence, so that the error can be controlled within a stable range.

After completing the compensation strategy, we let the end of the surgical instrument walk around the center of the workspace with a radius of $0.1m$. Fig. 4 (e)(h) are respectively the effect pictures before and after compensation, Fig. 4 (f)(i) are respectively the relative error along circle. Results show that maximum relative error reaches $0.7mm$ before compensation and $0.06mm$ after compensation. This magnitude of error is perfectly acceptable in surgery.

IV. Control Architecture

Several master slave motion control strategies are adopted to enhance the master slave control efficiency [12][13], they are hand-eye coordination, incremental motion control and proportional motion control [14][15]. Hand-eye coordination is also known as intuitive motion control, to realize intuitive motion control, the motion of the master manipulator must be described in the monitor coordinate system, Furthermore, the motion of the instrument must be described in the endoscope coordinate system [16][17], which can be described as:

$$ {}^{B}_{I}M = {}^{B}_{E}R \cdot {}^{E}_{M}R \cdot {}^{M}_{H}M \tag{12} $$

where ${}^{B}_{I}M$ denotes the desired motion of the instrument tip described in base coordinate system, ${}^{M}_{H}M$ denotes the motion of the endeffector of the master manipulator described in master coordinate, ${}^{B}_{E}R$ denotes the forward kinematics of the

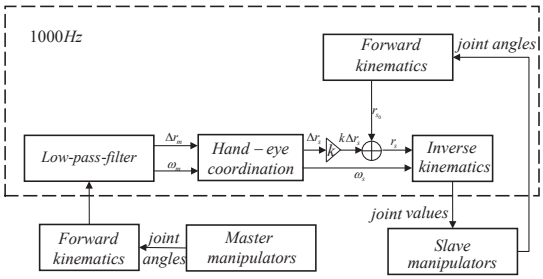

Fig. 5. Teleoperation process.

endoscope arm, ${}^{E}_{M}R$ denotes the transform matrix from master frame to monitor. The control framework is shown in Fig. 5, The joints control values generated by teleoperation run in cycle of 1ms, master manipulator generate teleoperation instructions in cartesian space, position and rotation are included. In order to filter out high frequency noise, a first-order low-pass filter with a cut-off frequency of 5 Hz is adopted. Proportional motion control is used to convert increment movement of the master manipulator into that of the slave manipulator. Proportional control is mainly used to improve the accuracy of surgery. Incremental control is mainly used to reposition the master manipulator during surgery, because the master manipulator may encounter the limits of motion, at this time, we can keep the slave manipulator in current position and restore master manipulator to zero position, then, the previous control process can be repeated. Δr_m and $\Delta \omega_m$ denotes the position increment and attitude of the master manipulator, respectively. Δr_s and $\Delta \omega_s$ denotes the position increment and attitude of the end-effector of the instrument. Δr_{s_0} and Δr_s denotes the actual position and the desired position of the instrument tip. k denotes the gain factor of the position increment. We set the value to 0.3 in the experiment. It is worth noting that attitude cannot be multiplied by gain k.

V. Simulation Scenes

In order to verify the effectiveness of the algorithm, three scenes were set up in the gazebo environment. Our gazebo simulator is composed of a SUJ, two PSMs and one ECM. The robotic arms have been modeled starting from the CAD models designed by team. For each manipulator we included the dynamic parameters obtained by CAD models, at the end of the endoscope, a depth camera has been included to simulate the binocular vision system of the real endoscope of "HuaTuo II". We set a resolution for the cameras at 800·800 pixels and the transmission frequency at 30Hz, because the model file is very large, therefore, considering a computer powered by a $IntelI9-8700$, $16GB$ of ram and $NvidiaGeForce1060$.

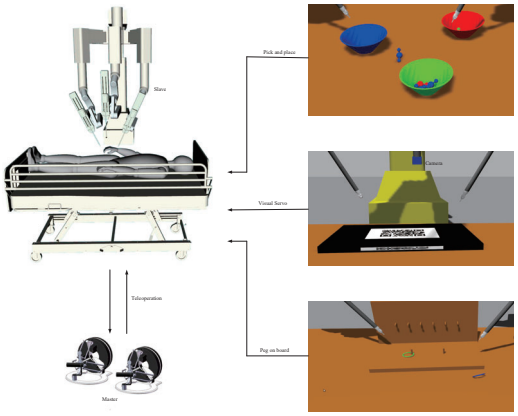

Fig. 6. Simulation scenes.

A. Dynamic Grasp

As is shown in Fig. 6, In the dynamic grabbing process, the value of parameter k can be set to 0.2 or 0.3 according to the actual operation requirements. The scenes have been realized by developing and importing CAD models of the training setup into the scene. Collision model and dynamical properties have been created through the SRDF file. The control architecture presented allows to easily interface the simulated robot with the master handles, like omega7. It is well known that simulation is very important since it can provide scores information about the surgeon skills. However, most simulators are costly and not completely exploitable by roboticists for research purposes. It is very convenient for us to implement advanced algorithm and training surgical skills through pick & place environment and Peg on board scenes.

B. Visual Servoing

In this section, a vision-based object tracking algorithm is proposed for "HuaTuo II" as a simple example. The task consists in autonomously regulating the pose of the ECM to track QR code, because due to actual surgical needs sometimes, we need to pay attention to the part of a feature in the operation, so we need to link the endoscope to the surgical features in real time. For simplicity we used a QR code. The tracking algorithm is implemented by VISP [18][19][20], VISP provides a set of visual features that can be tracked using real time image processing or computer vision algorithms. Hence, a QR code tracker has been implemented using VISP. the features on the QR code are extracted by the camera in real time, the target point position and attitude are calculated by the VISP algorithm. Then, we use the same principle as teleoperation to control the movement of the ECM. ECM has only three degrees of freedom, so its inverse kinematics is part of PSM, we will not repeat them here. After completing the above two simulation scenarios, we can easily develop

advanced algorithms and train surgical personnel.

VI. Conclusion and Future Work

In this work, a complete forward and inverse kinematic solution for "HuaTuo II" are provided and implemented. Then, the teleoperation algorithm is completed based on kinematics model. The errors that occurred in the establishment of the inverse kinematics model are analyzed in detail and the compensation measures are given. To show the advantages and potentialities of the proposed algorithm, we developed three different scenes in gazebo. On the other hand, the integration of our controller with ROS allows controlling the robot using the real master device and developing advanced control strategies. In future works, we will develop more advanced algorithm for "HuaTuo II".

Acknowledgment

This work was supported by National Key R&D Program of China ($No.2017YFC0110500$) and the Technological Innovation Program of the Science and Technology Commission of Shanghai Municipality ($No.16441908500$).

Appendix

The homogeneous transformation definition:

$$TransX(x) = \begin{bmatrix} 1 & 0 & 0 & x \\ 0 & 1 & 0 & 0 \\ 0 & 0 & 1 & 0 \\ 0 & 0 & 0 & 1 \end{bmatrix} RotX(x) = \begin{bmatrix} 1 & 0 & 0 & 0 \\ 0 & cos(x) & -sin(x) & 0 \\ 0 & sin(x) & cos(x) & 0 \\ 0 & 0 & 0 & 1 \end{bmatrix}$$

$$TransY(y) = \begin{bmatrix} 1 & 0 & 0 & 0 \\ 0 & 1 & 0 & y \\ 0 & 0 & 1 & 0 \\ 0 & 0 & 0 & 1 \end{bmatrix} RotY(y) = \begin{bmatrix} cos(y) & 0 & sin(y) & 0 \\ 0 & 1 & 0 & 0 \\ -sin(y) & 0 & cos(y) & 0 \\ 0 & 0 & 0 & 1 \end{bmatrix}$$

$$TransZ(z) = \begin{bmatrix} 1 & 0 & 0 & 0 \\ 0 & 1 & 0 & 0 \\ 0 & 0 & 1 & z \\ 0 & 0 & 0 & 1 \end{bmatrix} RotZ(z) = \begin{bmatrix} cos(z) & -sin(z) & 0 & 0 \\ sin(z) & cos(z) & 0 & 0 \\ 0 & 0 & 1 & 0 \\ 0 & 0 & 0 & 1 \end{bmatrix}$$

References

[1] Freschi, Ferrari V, Cinzia, et al. "Technical review of the da Vinci surgical Telemanipulator." The International Journal of Medical Robotics and Computer Assisted Surgery 9.4 (2013): 396-406.

[2] Chen, Zihan, et al. "Software architecture of the da Vinci Research Kit." 2017 First IEEE International Conference on Robotic Computing (IRC). IEEE, 2017.

[3] Yi, Bo, et al. "Domestically produced Chinese minimally invasive surgical robot system Micro Hand S is applied to clinical surgery preliminarily in China." Surgical endoscopy 31.1 (2017): 487-493.

[4] Wang, Wei, et al. "System design and animal experiment study of a novel minimally invasive surgical robot." The International Journal of Medical Robotics and Computer Assisted Surgery 12.1 (2016): 73-84.

[5] Marescaux, Jacques, and Francesco Rubino. "The ZEUS robotic system: experimental and clinical applications." Surgical Clinics 83.6 (2003):1305-1315.

[6] Intuitive Surgical, Inc. (2019) Investor presentation Q3 2019, https://isrg.gcs-web.com. Accessed October 1st 2019.

[7] Paul, Richard P. Robot manipulators: mathematics, programming, and control: the computer control of robot manipulators. Richard Paul, 1981.

[8] Zsombor-Murray, P. J. "Descriptive geometric kinematic analysis of clavels Delta Robot." Centre of Intelligent Machines, McGill University, USA (2004).

[9] Rosen, Jacob, et al. "Raven: Developing a surgical robot from a concept to a transatlantic teleoperation experiment." Surgical Robotics. Springer, Boston, MA, 2011. 159-197.

[10] Hayashibe, Mitsuhiro, et al. "Robotic surgery setup simulation with the integration of inverse-kinematics computation and medical imaging." computer methods and programs in biomedicine 83.1 (2006):63-72.

[11] Tang, Aolin, et al. "Motion Control of a MasterSlave Minimally Invasve Surgical Robot Based on the Hand Eye-Coordination." Computer Aided Surgery. Springer, Tokyo, 2016. 57-71.

[12] Wang, Ziheng, Isabella Reed, and Ann Majewicz Fey. "Toward intuitive teleoperation in surgery: Human-centric evaluation of teleoperation algorithms for robotic needle steering." 2018 IEEE International Conference on Robotics and Automation (ICRA). IEEE, 2018.

[13] Berthet-Rayne, Pierre, et al. "Inverse kinematics control methods for redundant snakelike robot teleoperation during minimally invasive surgery." IEEE Robotics and Automation Letters 3.3 (2018): 2501-2508.

[14] Ai Y, Pan B, Niu G, et al. Master-slave control technology of isomeric surgical robot for minimally invasive surgery[C]//2016 IEEE International Conference on Robotics and Biomimetics (ROBIO). IEEE, 2016: 2134-2139.

[15] Taylor R H, Menciassi A, Fichtinger G, et al. Medical robotics and computer-integrated surgery[M]//Springer handbook of robotics. Springer, Cham, 2016: 1657-1684.

[16] Itkowitz B D, DiMaio S P, Lilagan P E, et al. Method and system for hand presence detection in a minimally invasive surgical system: U.S. Patent Application 15/661,940[P]. 2017-11-9.

[17] Gao Y, Wang S, Li J, et al. Modeling and evaluation of handeye coordination of surgical robotic system on task performance[J]. The International Journal of Medical Robotics and Computer Assisted Surgery, 2017, 13(4): e1829.

[18] Hutchinson, Seth, and F. Chaumette. "Visual servo control, part i: Basic approaches." IEEE Robotics and Automation Magazine 13.4 (2006): 82-90.

[19] Hutchinson, Seth, Gregory D. Hager, and Peter I. Corke. "A tutorial on visual servo control." IEEE transactions on robotics and automation 12.5 (1996): 651-670.

[20] Espiau, Bernard, Franois Chaumette, and Patrick Rives. "A new approach to visual servoing in robotics." ieee Transactions on Robotics and Automation 8.3 (1992): 313- 326.